

VLT Laser Guide Star Monitor facility: a feasibility study

Pedichini F.^a, Ageorges N.^b, Sarazin M.^c

^aINAF Obs. Roma; ^bESO Chile, ^cESO Garching

ABSTRACT

The realtime knowledge of the altitude and optical characteristics of a generated Laser Guide Star may be necessary for an independent control of the performances of the associated adaptive optics system. For this purpose a robotic laser guide star monitoring facility, based on a small telescope physically separated from the observatory has been studied, as a subsystem of the VLT LGS project. After reviewing the state of the art on sodium layer dynamical characteristics, we describe the rationale of the project and the main technical choices. Some particular aspects such as differential field motion and laser plume centroiding algorithms are reviewed in detail. The data processing architecture and the associated pipeline is described, and the expected performances are estimated.

Keywords: Laser guide star, robotic telescope, sodium layer, pattern recognition

1. INTRODUCTION

1.1. The sodium layer

The sodium layer considered here is situated in the mesosphere at 91.5 ± 10 km and has a mean column density of $3 \times 10^9 \text{ cm}^{-2}$, value that is strongly latitude dependent. However this layer ‘suffers’ from seasonal, daily and short-term variations. The seasonal variations are ‘sinusoidal’ and affect the sodium column density, the average centroid position of the layer and its thickness (see e.g. ¹Papen et al. 1996). The sodium chemistry is known to be a sensitive function of temperature and the seasonal temperature variations appear to be largely responsible for the seasonal variations in the Na abundance which is maximum in winter (i.e. July-August in Chile). Papen et al. (1996) quote a mean sodium column density (at 40 degrees latitude North) of $4.3 \times 10^9 \text{ cm}^{-2}$ (with variations from 1 to $8 \times 10^9 \text{ cm}^{-2}$) and a mean layer altitude of 91.7 ± 2 km. Measurements of sodium column density presently available for La Silla show variations from 1 to $4.5 \times 10^9 \text{ cm}^{-2}$. Variations of the centroid position of the layer have a direct impact on the focus for laser guide star. ²Ageorges et al. (2000) quote variations of the centroid altitude position of the layer of up to 400m in 1 to 2 minutes (at 37 degrees North). For Laser Guide Star Adaptive Optics, the short-term variations of the atmospheric sodium are the most worrisome. These variations can be classified in two types: the daily and ‘hourly’ ones. Gravity waves are believed to be responsible for the daily modification of the Na layer, even though it is not yet clear how. Moreover ³Qian et al. (1998) conclude that these waves play an important role in the formation of sporadic Na layers (Na_s). These are very thin (0.5 to 2 km thick) Na layers superposed to the mean mesospheric sodium layers. They are characterized by a rapid increase in sodium density over a narrow altitude range. They can last few seconds but in average few minutes up to few hours. The ‘hourly’ variations of the mesospheric sodium layer, mentioned above, are clearly dominated by these sporadic layers. Sporadics have been detected more frequently at high and low latitude than mid-latitude sites. It has long been recognized that many Na_s are associated with sporadic E layers. It has therefore been suggested that the apparition of these layers might be related to magnetic latitude more than to geographic latitude (⁴Kwon et al. 1998). With the exception of ⁴Kwon et al. 1988, none of the other authors mentioning sporadics did see any ‘time’ correlation for their occurrence; neither does it appear to have significant seasonal difference in occurrence frequency. However many groups have measured enhancement of the sodium concentration during meteor showers (see e.g. ⁵Michaille et al. 2001). This can be understood since meteorite ablation is considered as the main source of mesospheric sodium. Sporadics Na layers will be the most affecting effect for LGS AO; see ⁶Clemesha et al. 1995 for a review of this still puzzling effect. Moreover, a sidereal motion is required for the LGS to follow the science object, which produces an horizontal displacement of the probed area in the sodium layer, and thus a possible increase of high frequency density variations which have to be studied.

1.2. Summary of important quantities

- Column density:
 - Mean : $3 \times 10^9 \text{ cm}^{-2}$
 - Range: $1-5 \times 10^9 \text{ cm}^{-2}$
 - Maximum (in case of sporadics): $12 \times 10^9 \text{ cm}^{-2}$
 - Effect of sporadic: multiply the mean value by 2 to 4 in average
- Centroid position of layer:
 - Mean altitude: 91.5 km
 - Variations: $\pm 2 \text{ km}$
- Modeling the sodium profile:
 - Density range: $0.1-12 \times 10^4 \text{ cm}^{-3}$
 - Shape: well approximated by a gaussian (possibly superimposed multiple gaussians in case of strong sporadics)
 - Temporal stability: $\sim 1 \text{ minute}$

2. SYSTEM STUDY

2.1. The LGSM principle

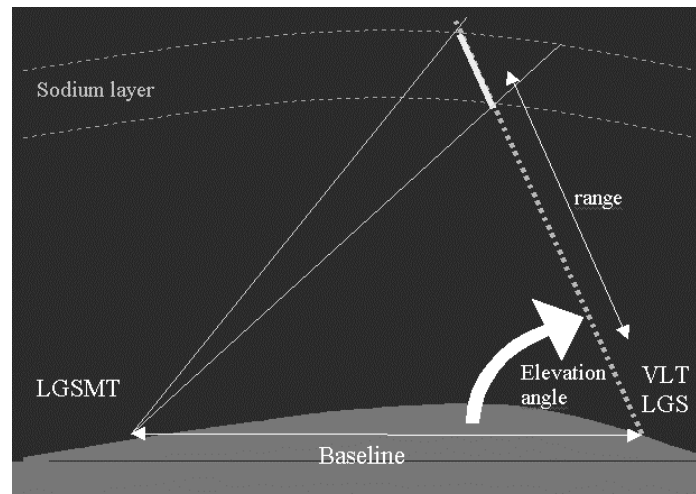


Fig. 1: Principle of the Laser Guide Star Monitoring System

The operational concept of the LGSM can be easily understood referring to Fig. 1 where the side looking principle of this device is described. A small telescope called LGSM T, located a few kilometers away from the LGS launching telescope, can take short exposures of the sky field where the sodium LGS is generated exciting the mesospheric Sodium layer. From the LGSM site the sodium star is recorded as a bright luminescent plume superimposed on a stellar field. After an exposure of about 30 sec, an automated software extracts the plume brightness profile from the recorded image. Using telescope encoders absolute positions, VLT pointing coordinates and stellar field analysis, the apparent brightness profile is then converted into relative sodium distribution abundance along the VLT LGS line of sight. The centroid position of the LGS is transmitted to the adaptive optics (AO) system to compensate for the defocus parameter. Subsequent analysis of the plume transversal PSF yields the position of the most populated areas of the sodium layer at which to conjugate the focus of the LGS launch telescope.

2.2. Simulations

In order to better estimate the performances of the LGSM simulation softwares have been created both in Excel and IDL to optimize all the free parameters of the instrument. These parameters are described in the following list:

DEFINITION OF TERMS

- Aperture:** LGSM telescope entrance pupil diameter, in m
- Focal Length:** LGSM telescope focal length, in m
- Pixel size:** detector pixel pitch, in arcsec
- Global Quantum Efficiency (QE):** conversion factor from photons to recorded ADU
- Field of view:** sky field in arcmin on the detector area.
- RON:** detector read out noise in e/pixel
- Gain:** camera controller conversion factor from electrons to ADU
- Exposure:** detector exposure time in seconds
- S/N:** signal to noise level per pixel along the laser plume (constant flat profile)
- Baseline:** distance on the ground between LGS launch telescope and LGSMT
- Range resolution:** projected pixel length along the LGSF laser path at the altitude of the Na layer, in m

For a given optical configuration, the range resolution depends on the elevation angle of the laser beam: the system must fulfill the top level resolution requirement with an LGS produced from zenith down to the lowest elevation of 30 degrees. The best range resolution is achieved with the LGS pointing around the zenith. At low elevation angles the perspective projection reduces the dimension of the laser plume on the focal plane of the LGSMT making it faster to record or increasing its S/N for a fixed exposure time with respect to zenith pointing. The following charts Fig.2 and 3 reports the result from simulations where the free parameters were the baseline and the telescope aperture while the focal length was arranged to yield the desired range resolution of 150 m. The exposure time was varied to reach a S/N of 15 enough to reduce the centroiding error due to photon noise to less than 1/5th of a pixel (Table 4). The desired data refresh time of about 30 seconds can be achieved with a limited aperture telescope (<40cm) only if the baseline is larger than 2 km (Fig. 2), especially when pointing where the LGS will be mainly used, ie. nearby the zenith. The results at the minimum elevation of 30 degrees are shown in Fig. 3: the S/N value of 15 is obviously reached faster when pointing at LGS with a lower elevation. Exposure times of about 20 –30 sec. are enough to detect a lot of field stars and other astronomical objects with a good S/N for precise astrometrical reduction of the imaged fields (see Table 1). Using on line astrometric catalogs, it will be possible to recognize the stellar field in few seconds and, by means of spherical trigonometry extract the ranging coordinates of the laser plume along the laser beam, using the Alt-Az pointing coordinates of the LGS launch telescope.

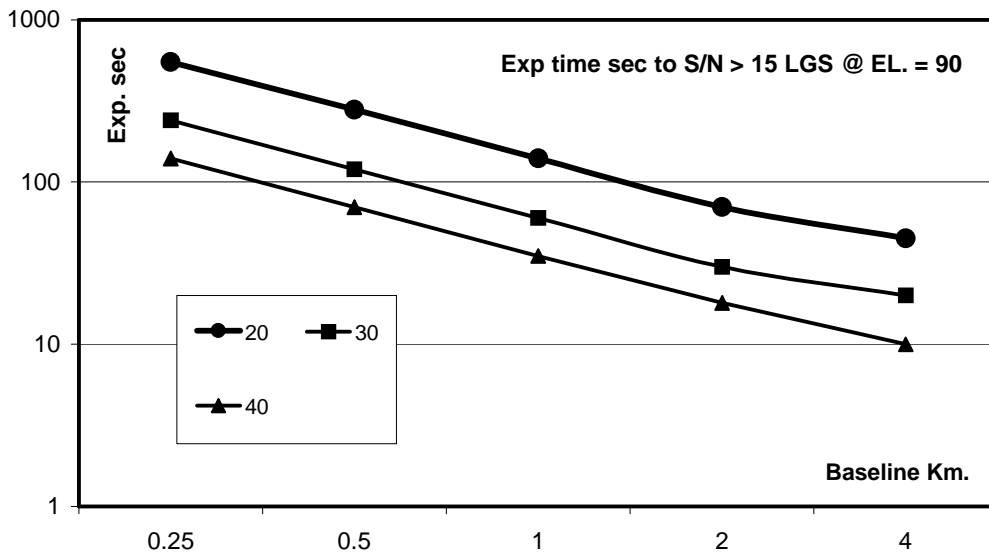


Fig. 2: Exposure time required to reach S/N=15 for an LGS at zenith. The detector camera parameters were the followings: Total Q.E. : 0.55, RON : 5 electrons, Pixel size :15 micron, CCD pixels : 1024 x 1024, Gain=0.33. The three lines represent different LGSM telescope apertures of 20, 30 and 40 cm.

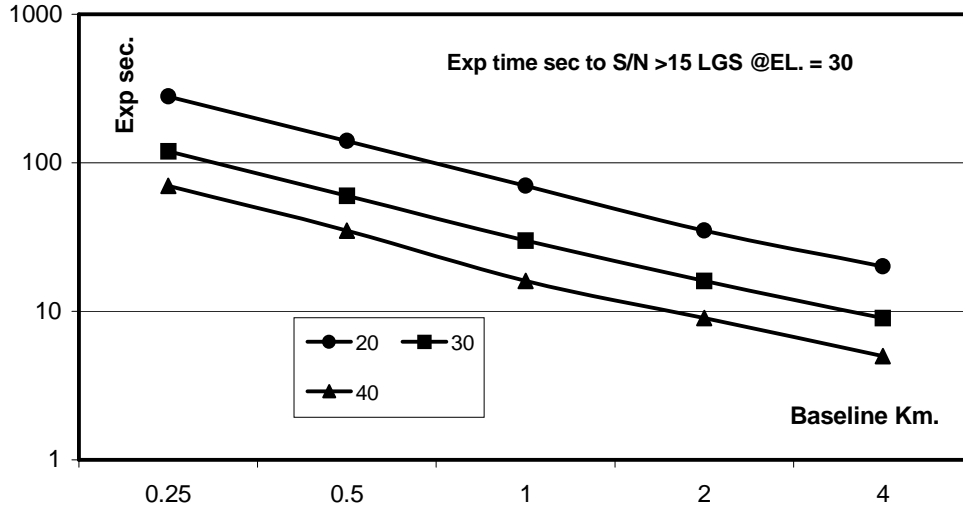


Fig. 3: Exposure time required to reach $S/N=15$ for an LGS at 60 degree zenith angle. The detector camera parameters were the followings: Total Q.E. : 0.55, RON : 5 electrons, Pixel size : 15 micron, CCD pixels : 1024 x 1024, Gain=0.33. The three lines represent different LGSMT telescope apertures of 20, 30 and 40 cm.

V magnitude	Number of stars
6	0.1
10	3.3
14	33
18	256
20	560

Table 1: The forecasted star density, for a 20 x 20 arcmin area, at high galactic latitude (less crowded areas) from ⁷Bahcall and Soneira (1983).

3. PROPOSED CONFIGURATION

3.1. Site Layout

The distance of the LGSMT to the LGSF launch site determines the size of the primary optics of the LGSMT, a major hardware cost component in the project: as shown on, the longer the separation, the smaller the telescope. On the other hand, the cost of underground communication lines increases with the distance up to a point where radio waves become preferable. The tradeoff shall be made at a later stage of the project. According to Figure 4 and taking into account existing infrastructure in the VLT science preserve, the summit of **La Montura** (intersection of lines 60 and 79 on Figure , 3.6 km from LGSF) is the preferred site. A second choice would be the vicinity of the so-called **NTT peak**, now the site of the **VISTA** telescope (intersection of lines 59 and 77, 1.4 km from LGSF), requiring less infrastructure developments, but at the cost a larger collecting area. The site of **La Montura** is known to be about 20% less windy than **Paranal/NTT peaks** with 93% of the time less than 10m/s (⁸VLT Report 62) but shows 10 to 20% worse seeing conditions. A tower and a small control room were built there in 1989 in the course of the VLT site survey. The range resolution achieved by the LGSMT located at **La Montura**, 3.6 km to the NE of the LGSF along the Na plume centered at 92 km above ground level, with the operating parameters of section 4.1 is given in Table 2 for various LGS elevations.

LGS Zenith Angle	Range resolution (m/px) 82km/92km/102km
0	11.3/14.2/17.4
20	13.9/17.5/21.4
40	26.1/32.7/40.0
60	93.2/116.8/143.1

Table 2: Performance of the LGSM at La Montura, 3.6 km from the LGSF

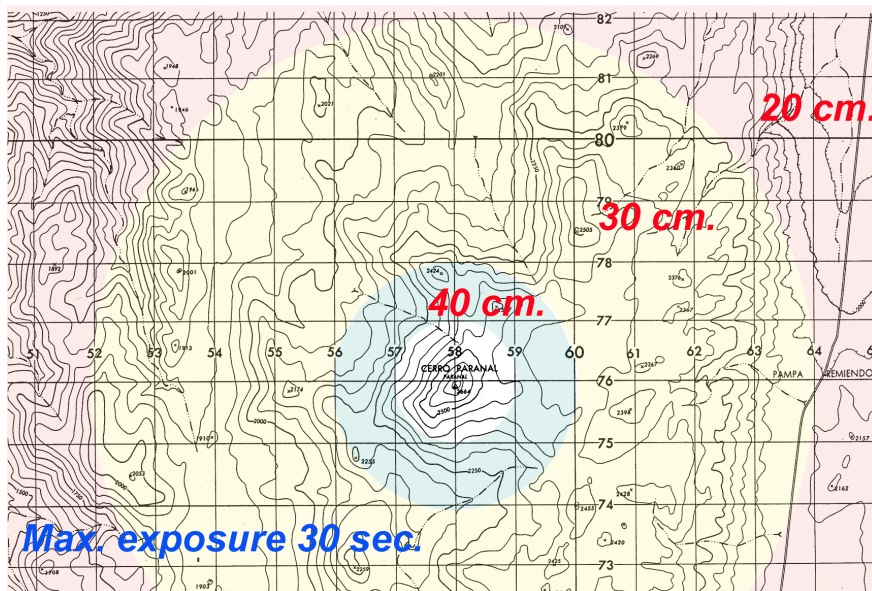


Figure 4: Telescope aperture required to achieve $S/N=15$ with a 30s exposure time on a zenith LGS as a function of the distance to the LGS launch site.

3.2. Operating Parameters

An IDL based end to end model has been developed to take into account non analytical effects, such as the differential motion of the laser plume versus the stellar field when observed off axis. The model is run with a "La Montura" configuration corresponding to a LGSM offset versus UT of 2km East, 3km North, and -0.2km in altitude, thus a baseline of 3.6km. The selected hardware configuration for the LGSM is the following:

- Telescope 30 cm aperture, focal length 250 cm
- Plate scale 1.238 arcsec/pixel
- Exposure 30 sec
- Detector characteristics: $QE=0.8$, $RON=5e$, $Gain=0.33$
- Focus: at the LGS altitude
- Field rotation compensation

Because of the parallax introduced when LGS and LGSM are not co-located, one should expect that the stellar background moves differently from the LGS as viewed from the LGSM. Two examples of real fields simulated when viewed from the proposed site are shown on Figures 5 and 6 for the same technical configuration, when the LGSM is tracking the LGS centroid. They illustrate the large variations in the relative motion of the background depending on the position of the LGS in the sky. It is believed however that astrometry is still possible in all cases because the blurring of the background is perfectly predictable.



Fig. 5: VLT pointing close to zenith: alfa 00 00 00 VLT, delta -24 00 00, hour Angle 00 00 00. LGSM at La Montura, exposure 30 s, seeing 1.2 arcsec, sky background 19.5, field size: 750x750 pixels.



Fig. 6: VLT pointing to the pole, alfa 00 00 00, delta -90 00 00, hour angle 00 00 00. LGSM at La Montura, exposure 30 s, seeing 1.2 arcsec, sky background 19.5, field size: 750x750 pixels.

3.3. Photometric optimization

With a laser plume recorded with the LGS at 45 degrees elevation viewed from a distance of 3.6 km from the launch site, a Johnson V filter of 90% peak transmission and 100 nm FWHM, the zenith LGS flux at the ground is $0.5 \cdot 10^6$ photons/sec/m² with an FWHM of 10 km at 92 km above ground level. With a 0.7 arcsec seeing and a 21st Mag V sky background, the pixel level at the peak of a V=17 star is 150 ADU and 700 ADU at the maximum of the LGS plume. The saturation (60000ADU) is reached for stars brighter than 9th magnitude, according to Table 1 each image should have at least one saturated pixel in the least populated area of the sky. With a plume covering at most 1000x3 pixels, the probability that one of them is saturated is then 3/1000. In the most crowded areas, this number rises to 1/100 in the galactic equator.

LGS Zenith Angle	S/N per pixel, Johnson V filter	S/N per pixel, D2 Filter
0	11	10
10	11	10
20	12	10
30	12	10
40	13	11
50	15	12
60	17	14

Table 3: Signal to noise achieved at the centroid of the Na plume with the proposed configuration and the operating conditions of. The signal to noise on a star of 15th Mag is 50.

It is possible to achieve 1/10th pixels astrometric accuracy with a minimum number of 3 useful objects in the field with a signal to noise per object greater than 20 (see Table 4). According to Table 1, there are more than three stars in the imaged field fainter than magnitude 10 in the least populated area. In the operating conditions, a S/N of 500 is reached on a 10th magnitude object. The image is assumed to be photon noise limited, which implies that the CCD dark current level and readout noise remain lower than the square root of the electron sky level (in dark nights: 64 e- for a 30s exposure with the proposed configuration). Adding a D2 filter is suggested to reduce star light contamination in crowded fields: a 10 nm FWHM interference filter of 50% peak transmission is equivalent to a loss of about 3.2 magnitudes with respect to the standard V filter. The S/N achieved with such a filter on the 10th magnitude object is then 127, fully within the astrometry requirements. The saturation magnitude range is then 5.8-6.3 and the S/N ratio achieved on the laser plume is given on Table . The sky background is then reduced to only 4 e- in a 30 s exposure and the dominant noise source is the camera. The simulation shows that the probability that one pixel of the plume is saturated becomes 3/10000 in the least crowded area of the sky and 15/10000 in the galactic equator.

Pixel S/N	Barycentric Centroiding error (px)
10	0.25
20	0.10
30	0.07
50	0.04
100	0.02

Table 4: Centroiding error due to image noise (photon, flat field, and readout noise) of a single pixel source.

3.4. Technical Specifications

The described LGSMT solution can be build mainly around industrial components to reduce the costs and the delivery time. The 30 cm, F# 8.3 optic must yield a distortion free focal plane covering a field of 20 arcmin. Both the Maksutov or the Ritchey Cretien designs can satisfy this requirement and are available from optical companies as off the shelf configurations. The constraint about the F# is not mandatory and a 10% tolerance can be well accepted. A stiff Alt. Az. mount (with derotator) implemented with sub arcsecond resolution encoders is mandatory for excellent pointing and

tracking performances needed for a fast and reliable automated astrometric reduction of the exposed field. The control system can be easily interfaced to the VLT LGS LAN by using a ESO LCU module with its software providing the bus connection to the boards required for the telescope motion, the camera controller and the dome opening. The standard ESO VLT software libraries will be implemented in the LCU for routine astrometric computations, the telescope pointing model and the on-line reduction and distribution of data. The dome itself can be selected between standard production housings for remote controlled small telescope preferring a sliding roof solution to avoid the control of the enclosure rotation. A list of technical specification is reported:

- Optical design : Ritchey Cretien or Maksutov telescope, with closed tube to minimize maintenance
Free distortion field : > 20 arcmin
Aperture : > 30 cm. (F# ~ 8.3)
Bandpass Filter: Johnson V (100 nm FWHM) & D2 (10nm FWHM, peak transmission > 50%)
- Mount type : ALT. AZ. with field derotation
Controls : brushless motors and sub-arcsecond on axes encoders
Slew speed : > 5 Deg./sec.
Tracking jitter : better than 0.2 arcsec for 1 minute in open loop
Mechanical stability: resonance frequency > 15Hz
- Camera : CCD with 1Kx1K pixel, V band enhanced (Q.E. > 85%)
r.o.n. < 5e-, dark current < 0.3 e⁻/pix/sec, Read out time : < 10 sec
frame transfer time < 10ms
cooling : maintenance free system (Peltier or cryo-cooler)

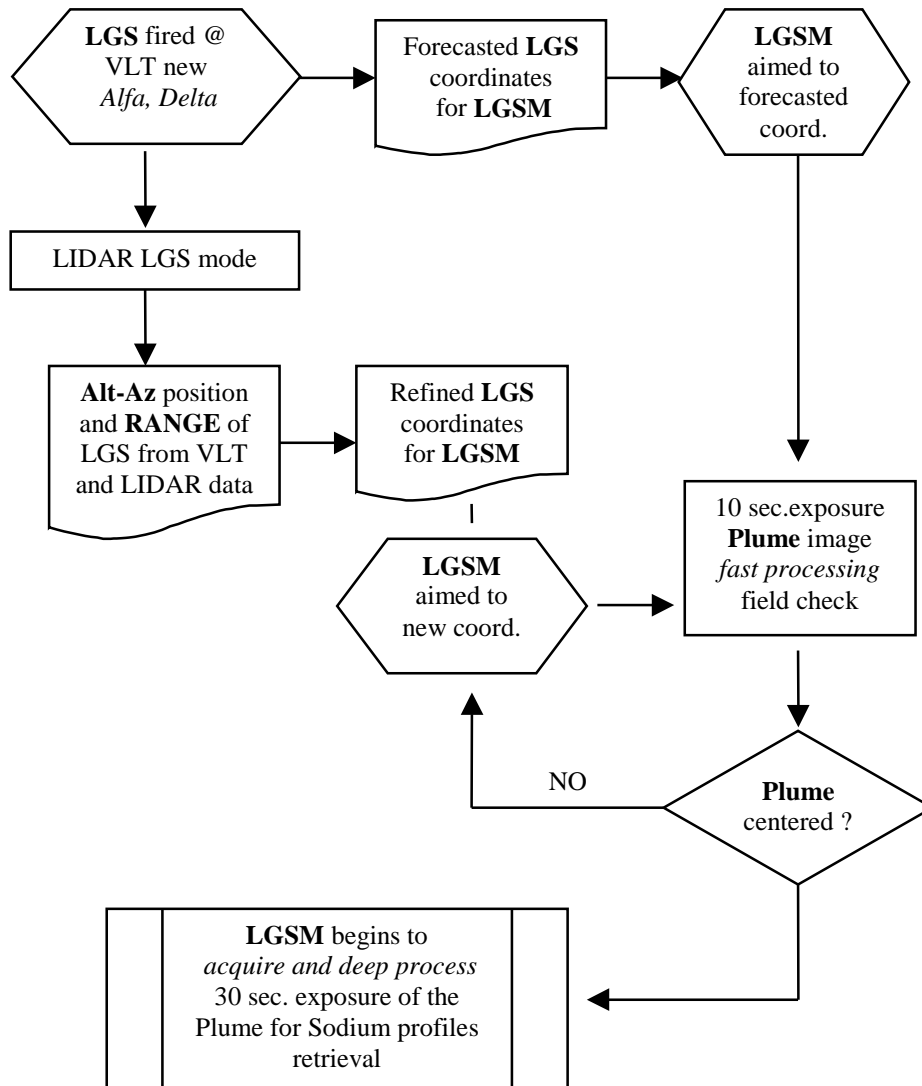
3.5. Operation

The LGSM is unattended and linked via LAN to the VLT backbone from which its main functions can be controlled (LGSM is in **MANUAL** mode) and its operational mode can be checked (LGSM in automated operation). The LGSM has permanent access to the VLT-ASM (Astronomical Site Monitor) meteorological data and to the VLT-UT alt-az coordinates. The LGSM is normally in **IDLE** mode (ready to operate, dome closed, checks the meteorological conditions and computes solar elevation every one minute, no hardware activity). At the reception of a <**WAKE-UP**> message from the LGSF containing target coordinates, the LGSM attempts to switch to **SLEW** mode (opens the enclosure and slews the telescope to the prescribed coordinates) if meteorology and solar elevation permit. Once the target coordinate is reached, the telescope is switched to tracking mode, the LGSM moves to **FIELD** mode, in which bright stars in the field are identified and the detector plate scale and sky coordinates are permanently updated. At the reception of a <**LIDAR**> message from the LGSF, containing the sodium layer initial abundance and profile, the LGSM switches to **MONITOR** mode, first scanning the field until the LGS appears, then in a 30 second infinite loop cycle, extracts the various LGS parameters, sends a <**LGSM DATA LOG**> back to LGSF and checks meteorology and applies tracking offsets. The loop is broken in the following circumstances:

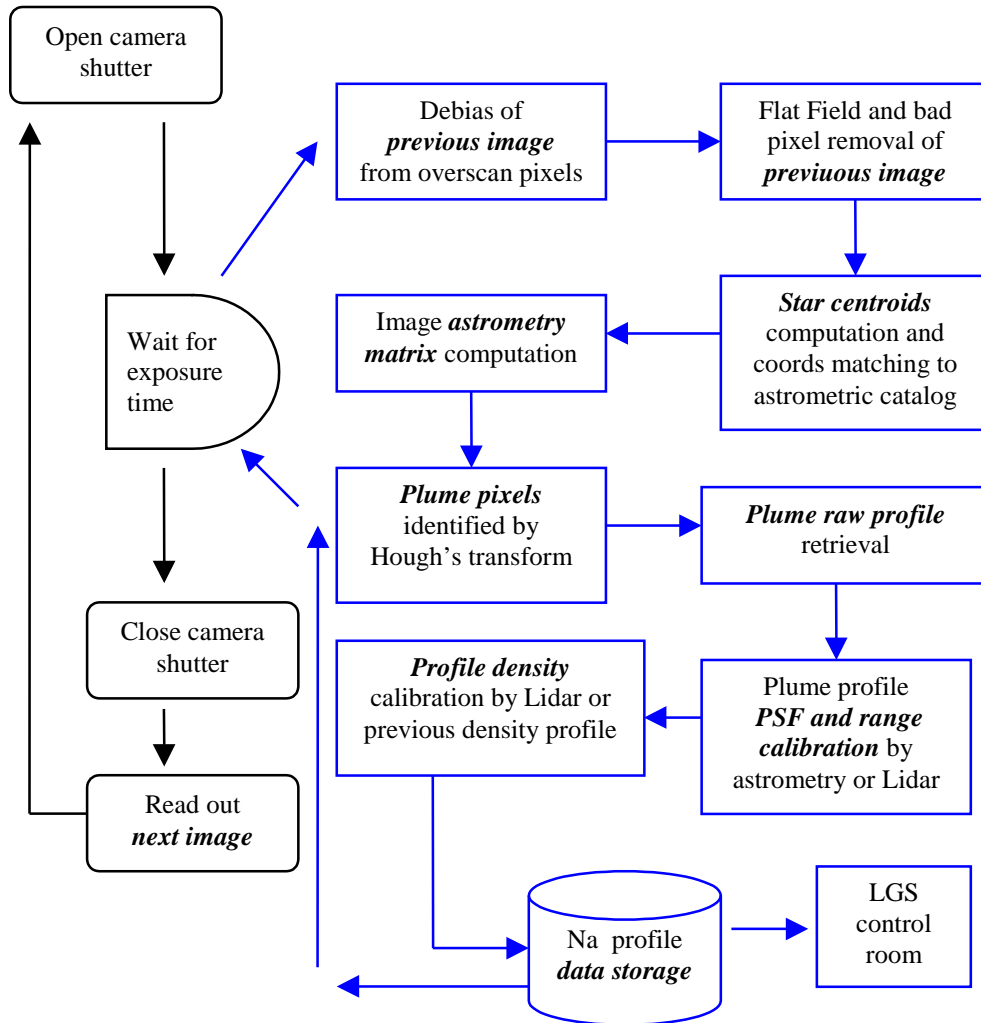
- When meteorological conditions exceed limit values, the system is then sent back to **IDLE** and tries to fulfill the current <**WAKE-UP**> call.
- At the reception of a new <**WAKE-UP**> message containing new target coordinates, the system is sent back to **SLEW** mode.
- At the reception of a <**SHUTDOWN**> message from the LGSF, indicating the end of operation, the current <**WAKE-UP**> call is then cancelled and the system is sent to **IDLE** mode.
- When the solar elevation exceeds its limit value, the system is then sent back to **IDLE** and the current <**WAKE-UP**> call is then cancelled.

4. DATA PROCESSING

4.1. Functional bloc diagram



4.2. Pipeline Description



The flow chart above shows the main tasks involved in the pipelined data reduction for the Sodium density profile retrieval. The exposure time of 30 sec. during each image acquisition will be used for the data processing of the previous acquired image. This means that each image is processed while the next image is exposed and acquired. To really exploit all the advantages of a pipelined data reduction is mandatory a strictly time scheduled software for the images processing always able to accomplish all the needed tasks before the shutter will be closed and the next image acquired. A brief description of the main tasks is following.

Debias and Flat-fielding

This is a standard astronomical image preprocessing task needed to remove noise due to the different pixels sensitivity of the CCD sensor. The calibration image (flat field) used is stored in the instrument database and has been acquired and computed during the last service/calibration run.

Star centroids

During this task the image is scanned to identify structures with a gaussian like shape above a flux threshold. Later on the identified stellar source the luminosity centroid is computed to refine their coordinates with sub-pixel resolution for

the cross correlation with an astrometric position catalog extracted from the GSC for the brightest sources inside the imaged area. Once the correlation has been performed at each source centroid will be attached its Equatorial Alfa Delta coordinates.

Astrometry

All the sources with attached Equatorial coordinates will be processed to compute an astrometry conversion matrix. With this output is possible to attach to each pixel or fraction of it in the image a couple of Alfa Delta or Alt. Az. coordinates needed for range determination.

Plume pixel extraction

In this phase the pixels belonging to the laser plume are be identified by using the Hough's transform. This peculiar algorithm extracts only the linear shapes returning the offset and angle of every line present in the analyzed field. The back transformation after the filtering in the Hough's space returns an image without stars with only the plume ready to be de-rotated by the plume angle. After this step the profile is ready to be extracted along the x and y-axes. The effect of the relative drift of the plume with respect to the reference stars (Figure 5) has to be studied in more details

Profile range calibration

Due to the perspective aberration of the plume the range coordinates along it do not follow a linear scale. The following trigonometric algorithm will set the range of each pixel of the plume. In the triangle AÛC we know the length AU, the angles CÂU and CÛA and we compute the lengths AC and

CU ($CAU = 90 - C\hat{A}E - U\hat{A}O$, $C\hat{U}A = 90 - F\hat{U}C - O\hat{U}A$). Finally $DU = CU / \sin (D\hat{U}C)$

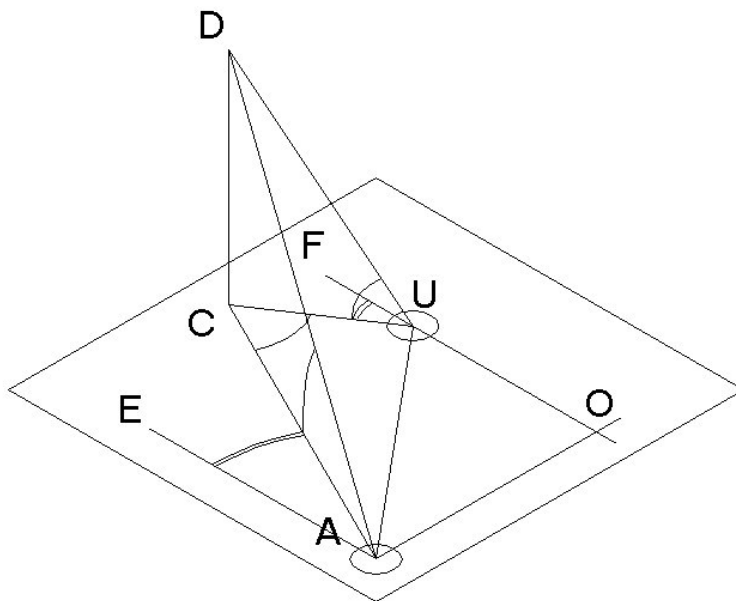


Figure 7: Geometrical definitions for an LGS in D , VLT in U and LGSM in A

Input: a) VLT pointing coordinates: azimuth FÛC & elevation DÛC, b) LGS centroid coordinates in the LGSM astrometric field: azimuth CÂE & elevation DÂC

Output: range DU of the centroid of the laser plume

Plume transverse characteristics measurements

The transversal sections of the laser plume will be used to check the focus of the LGS. Due to the relative under-sampling of the LGSM 1.23 arcsec/pixel to better extract its transversal PSF FWHM adjacent lines of pixel will be recentered and averaged exploiting the natural dithering of the plume itself on the CCD array. The effect of the plume broadening due to the relative drift of the plume with respect to the reference stars has to be studied in more details

LGS range determination

The centroid of the plume profile is computed as the light barycenter along LGSF line of sight, thus determining the LGS range.

4.3. Data storage

The sodium profiles and centroids are stored in the LGSF database. The photometric and astrometric parameters are stored locally (LGSM database) for self-check purposes and decision making on maintenance actions. One image per hour as well as all the images having generated an error code shall be stored for further inspection.

5. CONCLUSION

This paper shows how can be possible to monitor a LGS by means of an autonomous small robotic telescope sited few Km. away from the laser launch site. The original study performed by ESO and OAR includes also a budget forecast and a timeline for the building of the first prototype LGSM. This LGSM can be realized within 1 year of work applying about 2.5 FTE and then commissioned and fully tested in Paranal at the same time of the LGS first light.

REFERENCES

1. Papen G.C., Gardner C.S., Yu G., 1996; in: Adaptive Optics 13, OSA Technical Digest Series, Optical Society of America, Washington DC, p 96
2. Ageorges N., Redfern R. M., Delplancke F., O'Sullivan C., 2000, Proc. SPIE Vol. 4007, p. 384-394, Adaptive Optical Systems Technology, Peter L. Wizinowich; Ed.
3. Qian J., Gu Y., Gardner C.S., 1998, J. Geophys. Res. 103, 6333-6347
4. Kwon K.H., Senft D.C., Gardner C.S., 1988, J. Geophys. Res. 93, 14199-14208
5. Michaille L., Clifford J.B., Dainty J.C., Gregory T., Quartel J.C., Reavell F.C., Wilson R.W., Wooder N.J., 2001, MNRAS, submitted
6. Clemesha B.R., 1995, J. Atm. Terr. Phys. 57, 725-736
7. Bahcall J.N., Soneira R.M., ASSL Vol. 100, 1983, 209-216
8. VLT Report 62, VLT Site Selection Working Group Final Report, Nov.14, 1990, M. Sarazin Ed.